地震研究所彙報
Bull. Earthq. Res. Inst.
Univ. Tokyo
Vol. 76 (2001) pp. 271-289

Seismological Evidence for the Influence of Fluids and Magma on Earthquakes

Dapeng Zhao[1)]*, Om P. Mishra[1)], Ryohei Sanda[1)], Kazushige Obara[2)], Norihito Umino[3)] and Akira Hasegawa[3)]

[1)] Geodynamics Research Center, Ehime University
[2)] National Research Institute for Earth Science and Disaster Prevention
[3)] Research Center for Prediction of Earthquakes and Volcanic Eruptions, Tohoku University

Abstract

In this paper we present seismological evidence for the influences of fluids and arc magma on the generation of large earthquakes in the crust and the subducting oceanic slabs under the Japan Islands. The relationship between seismic tomography and large crustal earthquakes (M 5.7-8.0) in Japan during the period of 116 years from 1885 to 2000 is investigated, and it is found that most of the large crustal earthquakes occurred in or around zones of low seismic velocity. The low-velocity zones may represent weak sections of the seismogenic crust. Crustal weakening is closely related to the subduction process in this region. Along the volcanic front and in back-arc areas, crustal weakening may be caused by active volcanoes and arc magma, resulting from the convective circulation process in the mantle wedge and dehydration reactions in the subducting slab. Recent examples are the 1984 West Nagano earthquake (M 6.8) and the 2000 West Tottori earthquake (M 6.9), both occurred adjacent to volcanoes. In the forearc region of southwest Japan, fluids are detected in the 1995 Kobe earthquake source zone, which may have contributed to the rupture nucleation. The fluids may originate from the dehydration of the subducting Philippine Sea slab. The recent 2001 Geiyo earthquake (M 6.4) occurred at 50 km depth within the subducting Philippine Sea slab, and it may also be related to the slab dehydration process. A detailed 3-D velocity structure is determined for the northeast Japan forearc region using data from 598 earthquakes that occurred under the Pacific Ocean with hypocenters well located with sP depth phases. The results show that strong lateral heterogeneities exist along the slab boundary, which may represent asperities and results of slab dehydration, and may affect the degree and the extent of interplate seismic coupling. These results indicate that large earthquakes do not strike anywhere, but only in anomalous areas that may be detected with geophysical methods. The generation of a large earthquake is not a pure mechanical process, but is closely related to the physical and chemical properties of materials in the crust and upper mantle, such as magma and fluids.

Key words : fluids, magma, earthquakes, seismic tomography, slab dehydration

1. Introduction

A growing body of evidence suggests that fluids (water, magma, and gases such as CO_2 and SO_2) are intimately linked to a variety of earthquake faulting processes. These include nucleation, propagation, arrest, and recurrence of earthquake ruptures, fault creep or slow earthquakes, and the long-term structural and compositional evolution of fault zones. Besides the widely recognized physical role of fluid pressures in controlling the strength of crustal fault zones, it is also apparent that fluids can exert a mechanical influence through a variety of chemical effects. Fluids also play important roles in the dynamics and the evolution of the Earth, such as lowering the melting temperature of the mantle, transporting elements, enhancing diffusion and creep, and possibly changing the location of the phase boundary.

* e-mail : zhao@sci.ehime-u.ac.jp (2-5, Bunkyo-cho Matsuyama 790-8577 Japan)

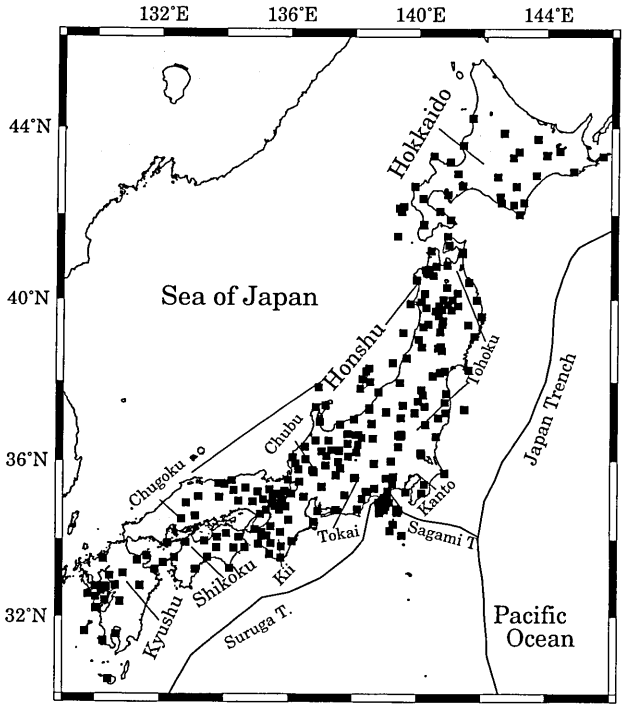

Fig. 1. Distribution of seismic stations of the *Japan University Seismic Network* (solid squares). Curved lines show the Japan Trench, Sagami Trough, and Suruga Trough, which are the major plate boundaries in the Japanese region.

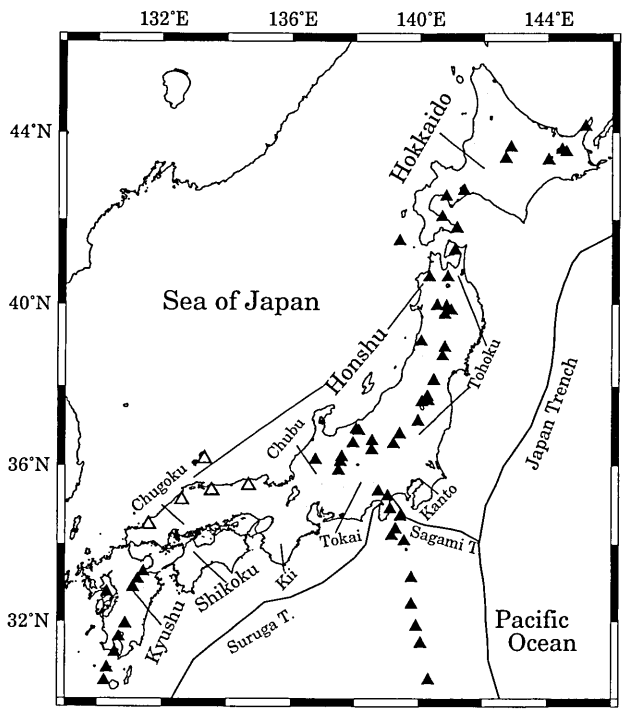

Fig. 2. Distribution of active volcanoes (solid triangles) and Quaternary volcanoes (open triangles) on the Japan Islands. Curved lines show the Japan Trench, Sagami Trough, and Suruga Trough, which are the major plate boundaries in the Japanese region.

In this paper we synthesize the seismological evidence (in particular, tomographic images) revealed so far to illustrate the influences of fluids and arc magma on the generation of large earthquakes in the crust and the subducting oceanic slabs under the Japan Islands. Japan is a country that has suffered greatly from seismic hazards during its long history. Nearly one tenth of the earthquakes on Earth occur in or around the Japan Islands, which are caused by active subduction and collisions among four lithospheric plates in this region (Ishida, 1992; Seno *et al.*, 1993, 1996). The Pacific plate is subducting from the east beneath the North America and Eurasian plates in eastern Japan; the Philippine Sea plate is descending from the south beneath the Eurasian plate in southwest Japan. Large interplate earthquakes occur frequently along the plate boundaries off the Pacific coast of the Japan Islands. Intraplate earthquakes within the continental plate take place in the upper crust beneath the Japan Islands and along the coast of the Japan Sea. Although the crustal intraplate earthquakes do not occur as frequently as the interplate earthquakes, they generally inflict greater damage, because they are shallow and near densely populated areas. Recent examples of inland crustal earthquakes are the 1995 Kobe earthquake (M 7.2) and the 2000 West Tottori earthquake (M 6.9).

Detailed tomographic images of the Japan subduction zone have been determined using a large number of arrival times from local, regional, and teleseismic events recorded by the dense *Japan University Seismic Network* (Fig. 1) (Zhao *et al.*, 1992, 1994, 2000a, b). The network is operated by eight national universities in Japan and consists of over 300 seismic stations equipped with short-period and broad-band seismographs (Tsuboi *et al.*, 1989). It densely and uniformly covers all of the Japan Islands with an average spacing between stations of 25–40 km. In addition to first P and S arrivals, we also picked about 1400 P to S and S to P converted waves at the upper boundary of the subducting Pacific plate and S to P converted waves at the Moho discontinuity (Zhao *et al.*, 1997a). We also picked 12,759 P wave arrival times from 174 teleseismic events (M 6.0–8.0) with epicentral distances from 30° to 90° (Zhao and Hasegawa, 1994; Zhao *et al.*, 1994, 2000a). The hori-

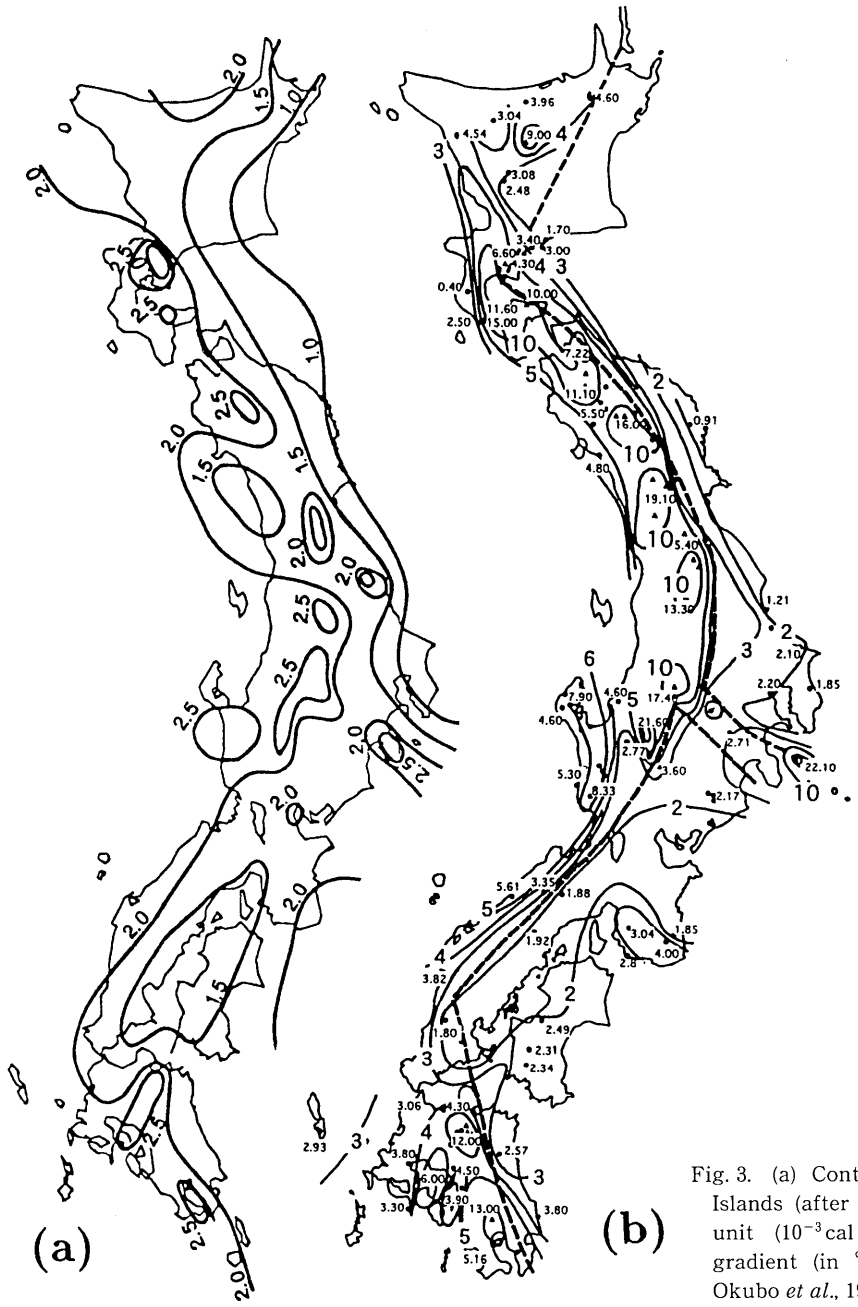

Fig. 3. (a) Contour map of heat flow on the Japan Islands (after Yuhara, 1973). Values are in heat flow unit (10^{-3}cal cm^{-3}s^{-1}). (b) Vertical geothermal gradient (in °C/100 m) on the Japan Islands (after Okubo *et al.*, 1989).

zontal resolution of tomographic images in Japan is 25 to 35 m for the crust and mantle wedge, and 35 to 40 km for the subducting Pacific and Philippine Sea slabs and the mantle below it. The vertical resolution is 10 to 30 km.

Active arc volcanoes exist in Hokkaido, eastern Honshu, and Kyushu (Fig. 2), which are associated with the subduction of the Pacific and the Philippine Sea plates (Yokoyama *et al.*, 1987). Quaternary volcanoes exist along the coast of the Japan Sea in Chugoku, which are also associated with the subduction of the Philippine Sea plate. These volcanic areas exhibit high heat flows and large geothermal gradients, indicating magma chambers beneath the volcanoes, so they have high temperatures (Yuhara, 1973; Okubo *et al.*, 1989) (Fig. 3). Our tomographic images show that seismic velocity is very slow in the volcanic areas, which is mainly caused by high temperatures (Fig. 4, 5). In Kii and Shikoku, there is no volcano and heat flows and geothermal gradients are low (Fig. 2, 3), suggesting that those areas have lower temperatures, and magma chambers may not exist.

2. Earthquakes in volcanic areas: Influence of arc magma

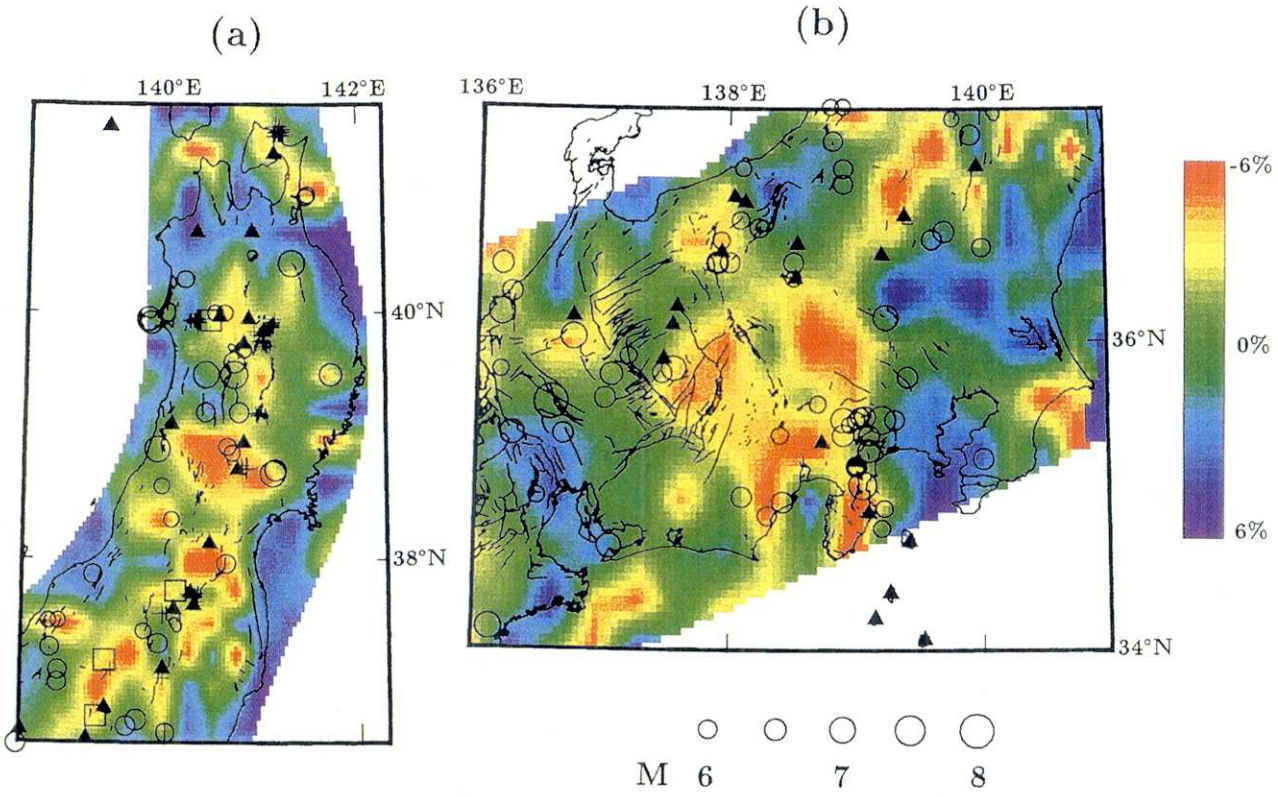

Fig. 4. P-wave velocity image at a depth of 40 km beneath northeast (a) and central Japan (b). Red and blue colors denote low and high velocities, respectively. Circles denote earthquakes (M 5.7-8.0, depths 0-20 km) that occurred during a period of 116 years from 1885 through 2000. Solid triangles denote active volcanoes. Active faults are shown by thick lines. The velocity perturbation scale and the earthquake magnitude scale are shown on the right and at the bottom, respectively. Crosses and open squares in (a) show low-frequency microearthquakes and S-wave reflectors in midcrust, respectively.

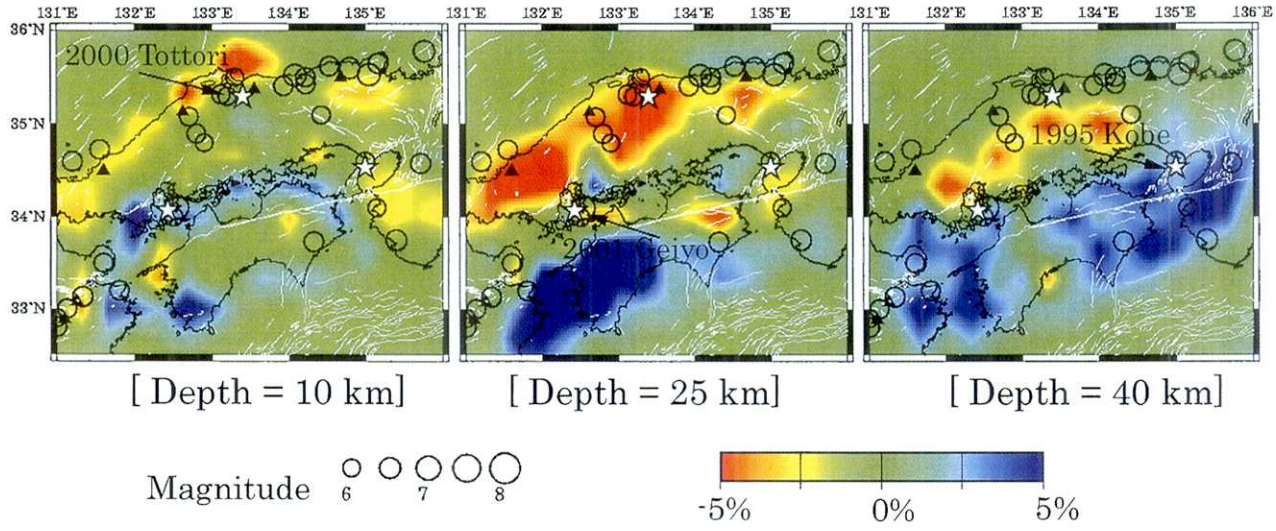

Fig. 5. P-wave velocity image at a depth of (a) 10, (b) 25, and (c) 40 km beneath southwest Japan. Solid triangles denote volcanoes. The star symbols denote the epicenters of the 1995 Kobe earthquake (M 7.2), the 2000 West Tottori earthquake (M 6.9), and the 2001 Geiyo earthquake (M 6.4). Other labelings are the same as Figure 4.

2. 1. Distribution of large earthquakes and tomography

The tomographic images are compared to active faults and 161 earthquakes with magnitudes of M 5.7 to 8.0 that occurred in the depth range of 0 to 20 km during a period of 116 years from 1885 through 2000 (Fig. 4, 5). Hypocentral locations and magnitudes of the large earthquakes are taken from Utsu (1982) and Usami (1999). Their earthquake catalogs are complete at the $M>5.7$ level. The accuracy of the hypocentral locations is estimated to be about 10 km for earthquakes until 1960 and about 5 km for events thereafter. The accuracy of the magnitudes is 0.2–0.3 for earthquakes until 1960 and 0.1–0.2 for the events thereafter. Because all of the large historic earthquakes used in this study occurred beneath the inland areas, their locations and magnitudes were relatively well determined.

We computed P-velocity perturbations ($\Delta V/V$) in the crust and uppermost mantle at the epicenters of the 161 large historic earthquakes in Japan and found that for 70% of the earthquakes, $-3\% < \Delta V/V < 0\%$, and 11% of them having $\Delta V/V < -3\%$. For the remaining 19% of large earthquakes, $0\% < \Delta V/V < 1.5\%$. These results indicate that large historic earthquakes generally occurred at the edge portion of low-V zones or along the boundary between low- and high-velocity bodies (Fig. 4, 5). Only some smaller events (M 5.7–5.8) are located in the central part of the low-V zones. It was noticed earlier that large earthquakes ($M>6.0$) do not occur within 10 km of a volcano (Ito, 1993). A few of the earthquakes are located in high-velocity (high-V) areas; those events are generally smaller than M 6.0. Note that the resolution of our tomographic images is 25 to 33 km in the horizontal direction and 10–15 km at depths in the crust and uppermost mantle. There is a possibility that some low-V and high-V zones smaller than the resolution scale may not be detectable in our current tomographic maps.

Zhao (2001) compared the tomography to the distribution of large crustal earthquakes that occurred during a period of 1,322 years from AD 679 to 2000 in Japan, and found the same pattern: most of the large crustal earthquakes are located in or around the low-V zones in the crust and uppermost mantle.

2. 2. Geophysical indicators of arc magma

In Tohoku (Fig. 4a), low-frequency microearthquakes occur in or around the low-V zones, which are caused by the upward intrusion of magma chambers (Hasegawa and Zhao, 1994; Hasegawa and Yamamoto, 1994). A total of 153 low-frequency microearthquakes during July 1976 to July 1991 were detected in the depth range of 22 to 47 km around the Moho discontinuity. These events have anomalously low predominant frequencies (1–5.5 Hz) for both P and S waves, in contrast to those (8–20 Hz) of normal crustal events (depths 0–15 km) in the brittle seismogenic layer. The magnitudes of these events are small ($M \leq 2.2$). The proximity of these events to the active volcanoes and the low-V zones in the uppermost mantle suggests that these deep, low-frequency microearthquakes are generated by magmatic activity of mantle diapirs.

S-wave reflectors are detected in the crust and they are also located in or around the low-V zones in volcanic areas (Matsumoto and Hasegawa, 1996; Horiuchi *et al.*, 1997) (Fig. 4a). Reflectors with a thickness of only about 100 m were detected in the mid-crust below the brittle seismogenic layer. They generated reflected S waves with anomalously large amplitudes, which can be explained by a large velocity contrast across a discontinuity underlain by very low-rigidity materials, such as magma or water in a super critical fluid state (Matsumoto and Hasegawa, 1996).

Attenuation tomography imaged high attenuation (low-Q) zones in the crust and mantle wedge beneath active volcanoes (Sekiguchi, 1991; Tsumura *et al.*, 2000). The Q images have a resolution of about 40 km. The low-Q zones coincide with the low-V zones (Fig. 4) in both location and spatial extent. In addition, seismic waves passing through the mantle wedge low-V/low-Q zones show strong shear wave splitting, indicating that the low-V/low-Q zones are very anisotropic (Iidaka and Obara, 1994; Okada *et al.*, 1995; Hiramatsu *et al.*, 1998). The origin of anisotropy in the low-V/low-Q zones is thought to be partial melting. The fraction of melts is estimated to be 2% from the degree of anisotropy and the velocity reduction.

Taking into account the coincidence of the active volcanoes, low-V/low-Q and anisotropic zones, low-frequency microearthquakes and crustal S-wave reflectors, the low-V zones in the uppermost

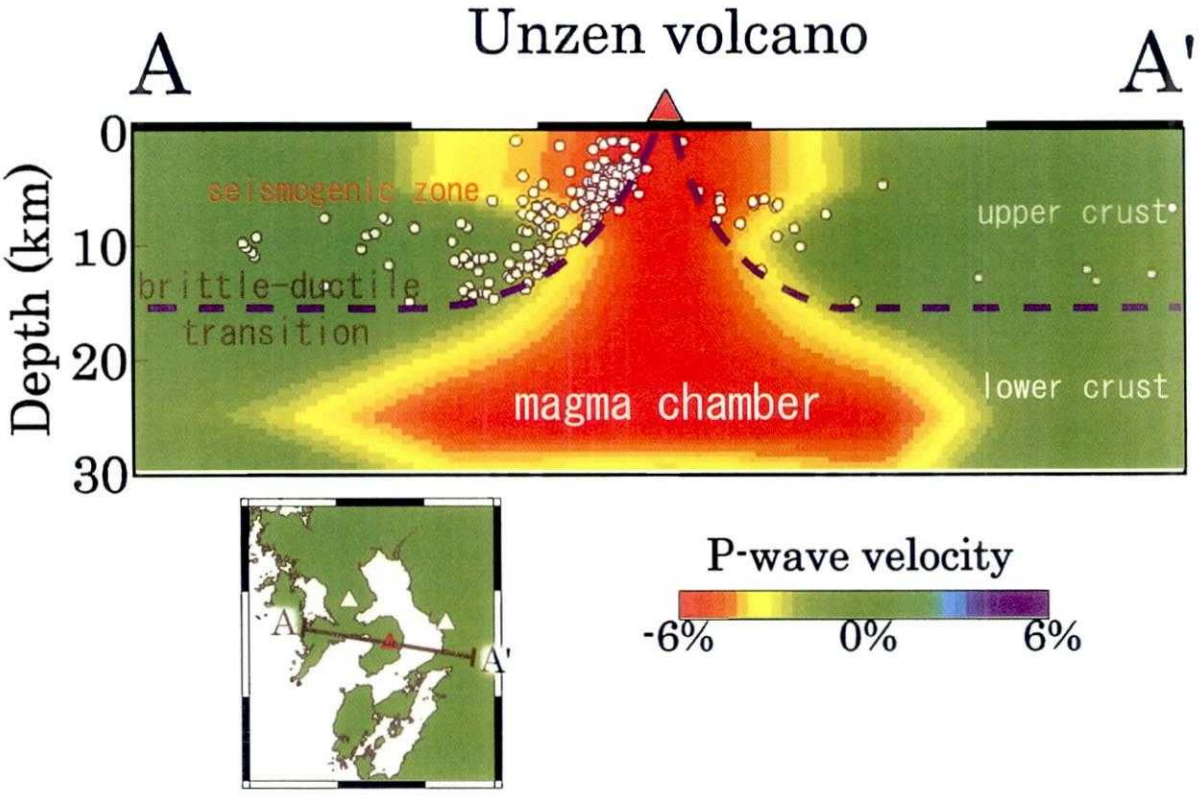

Fig. 6. East-west vertical cross-section of P-wave tomography of the crust under Unzen Volcano in Kyushu. Red and blue colors denote low and high velocities, respectively. The velocity perturbation scale is shown at the bottom. The dashed lines show the cut-off depth of crustal earthquakes (white circles). In the insert map the red triangle shows Unzen Volcano, white triangles denote other active volcanoes.

mantle (Fig. 4, 5) are interpreted to represent the magma bodies that form the source zone of the arc magmatism and volcanism (Zhao *et al.*, 1992, 1994; Hasegawa and Zhao, 1994). The volcanic areas underlain by the low-V zones generally have high topography and larger contractive crustal strain ($>10^{-5}$) in the plate convergence directions (Hasegawa *et al.*, 2000).

There are large lateral variations in the temperature of the crust and the cut-off depth of microearthquakes in the volcanic areas (Ito, 1993; Hasegawa *et al.*, 2000; Zhao *et al.*, 2000a). A typical example is that beneath Unzen Volcano in northern Kyushu (Fig. 6) (Asamori and Zhao, 2001). A cone-shaped low-V zone exists in the crust under Unzen Volcano, which may represent high-temperature anomalies containing melts or partial melts. This tomographic image is generally consistent with previous seismic and gravity studies in this region (e.g., Komazawa and Kamata, 1985; Suyehiro, 1988; Iidaka *et al.*, 1993; Ohmi and Lees, 1995). The cut-off depth of crustal microearthquakes becomes clearly shallower toward the crater of the volcano, and is in good agreement with the upper boundary of the low-V zone (Fig. 6). These features indicate a thinning of the brittle seismogenic layer beneath the volcano.

2. 3. Arc magma and large crustal earthquakes

A qualitative model is proposed to explain these observations for volcanic areas (Fig. 7). The low-V zones in the uppermost mantle (Fig. 4, 5) may be a manifestation of mantle diapirs associated with the ascending flow of subduction-induced convection in the mantle wedge and dehydration reactions in the subducting slab (Zhao *et al.*, 1992, 1997b). As mentioned above, magma rising further from the mantle diapirs to the crust may cause low-frequency microearthquakes at levels of the lower crust and uppermost mantle, and make their appearance as S-wave reflectors at midcrustal levels. Their upward intrusion raises the temperature and reduces the seismic velocity of crustal materials around them, causing the brittle seismogenic layer above them to become locally thinner and weaker.

Subject to the horizontally compressional stress

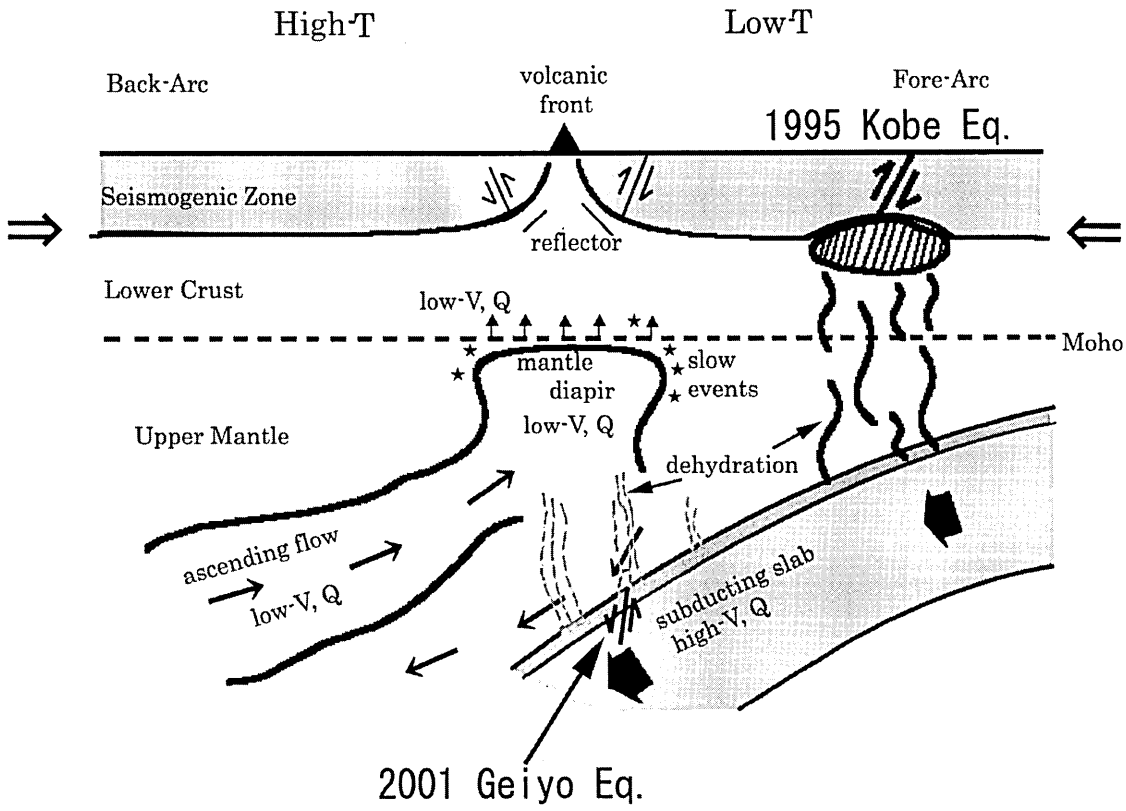

Fig. 7. Schematic illustration of across-arc vertical cross-section of the crust and upper mantle under a subduction zone region. Two processes are considered to be important: one is the corner flow in the mantle wedge, the other is the dehydration of the subducting oceanic crust at the top of the subducting slab. In the forearc region, the temperature is lower, and hence magma cannot be formed. The fluids from the slab dehydration may migrate up to the crust. If the fluids enter an active fault, pore pressures will increase and fault zone friction will decrease, which may trigger large crustal earthquakes. Under the volcanic front and back-arc regions, the temperature is high because the mantle wedge corner flow brings in the hot materials from the deeper mantle. Slab dehydration may contribute to the generation of arc magma. Migration of magma up to the crust produces arc volcanoes and causes lateral heterogeneities and weakening of the seismogenic upper crust, which can affect the occurrence of large crustal earthquakes.

field in the plate convergence direction, contractive deformations take place mainly in the low-V, low-Q areas because of the thinner brittle seismogenic layer and the weaker crust and uppermost mantle, due to the higher temperature and the existence of magma- or fluid-filled, thin, inclined reflectors that are incapable of sustaining the applied shear stress. The deformation proceeds partially in small earthquakes but mainly in plastic deformation, causing crustal shortening, upheaval and mountain building (Hasegawa *et al.*, 2000). Large crustal earthquakes cannot occur within the weak low-V zones, but can occur in edge portions where the mechanical strength of the materials is higher than those of the low-V zones, but is still weaker than the normal sections of the seismogenic layer. Thus the edge portion of the low-V areas becomes the ideal location to generate large earthquakes that produce faults reaching the Earth's surface or blind faults within the brittle upper crust (Fig. 7.).

3. Earthquakes in non-volcanic areas: Influence of fluids

Figure 5 shows a comparison of the distribution of large crustal earthquakes with the velocity images of the crust and the uppermost mantle in southwest Japan. The velocity images in the upper crust (Fig. 5a) are consistent with the surface geology. The high-velocity zones in Kii Peninsula and Shikoku at 25 and 40 km depths are associated with the subducting Philippine Sea slab. We can see that many of the large earthquakes occurred along the Japan Sea

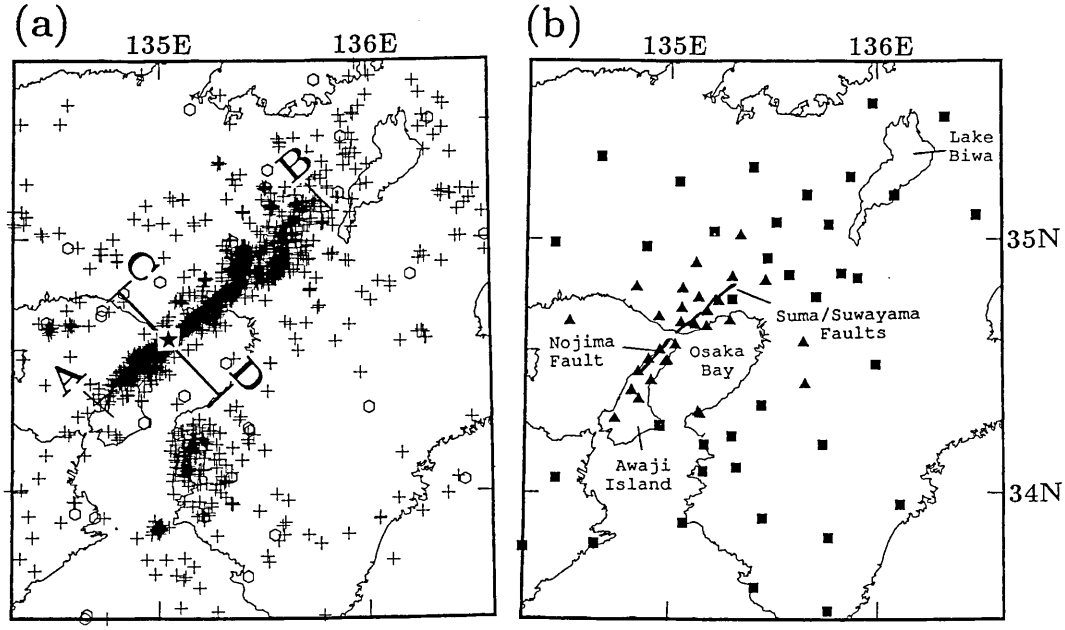

Fig. 8. (a) Epicentral distribution of 3,634 events used in the tomographic imaging of the source area of the 1995 Kobe, Japan, earthquake (star). Crosses denote the events that occurred after 17 January, 1995; most of them were aftershocks of the Kobe earthquake along the fault zone (parallel to cross section line A-B). Circles denote microearthquakes that occurred from January 1990 to December 1994. (b) Distribution of seismic stations that recorded the earthquakes in (a). Solid triangles denote portable stations that were set up following the Kobe mainshock. Solid squares denote permanent stations. Solid lines represent the surface traces of the Nojima, Suma, and Suwayama faults.

coast of Chugoku, where Quaternary volcanoes exist and seismic velocities are lower. These large earthquakes may have the same cause as that in the active volcanic regions (Fig. 4.). In Kii, Shikoku, and southern Chugoku, prominent low-V zones are visible, and large crustal earthquakes occurred also in or around the low-V zones. But it is difficult to attribute such low-V zones to high temperature because no volcano exists and heat flows and geothermal gradients are low in those non-volcanic areas (Fig. 2, 3).

3. 1. Fluids in the 1995 Kobe earthquake source

To unravel the cause of large earthquakes in the non-volcanic areas, we have made detailed investigations of the 1995 Kobe earthquake (M7.2), which may be representative of large crustal earthquakes in southwest Japan. Zhao *et al.* (1996) and Zhao and Negishi (1998) determined high-resolution 3-D P and S wave velocity and Poisson's ratio structures in the Kobe source area, and relocated the aftershocks with the 3-D velocity model obtained. They used 64,337 P and 49,200 S wave high-quality arrival times from 3,634 Kobe aftershocks and local microearthquakes recorded by over 100 permanent stations and 30 portable stations that were set up following the Kobe mainshock (Fig. 8.). The velocity models have a spatial resolution of 4-5 km in the Kobe fault zone.

Significant velocity variations of up to 6% are revealed in the aftershock area. The Kobe mainshock hypocenter is located in a distinctive zone characterized by low P and S wave velocities and high Poisson's ratio (Fig. 9). This anomaly exists in the depth range of 16 to 21 km, and extends 15 to 20 km laterally. This anomaly is interpreted to be a fluid-filled, fractured rock matrix, which contributed to the initiation of the Kobe earthquake. This interpretation has been supported by many pieces of evidence from hydrological, geochemical, seismological, and geophysical investigations conducted in the Kobe earthquake region (for details, see Zhao and Negishi, 1998).

There may be two origins of fluids in the Kobe fault zone: one is shallow origins such as meteoric water, pore fluids, and mineral dehydration in the crust (Kerrich *et al.*, 1984); the other is deep origins such as the dehydration of the subducting oceanic plate.

3. 2. Shallow origins of fluids

Zhao and Mizuno (1999) estimated the crack den-

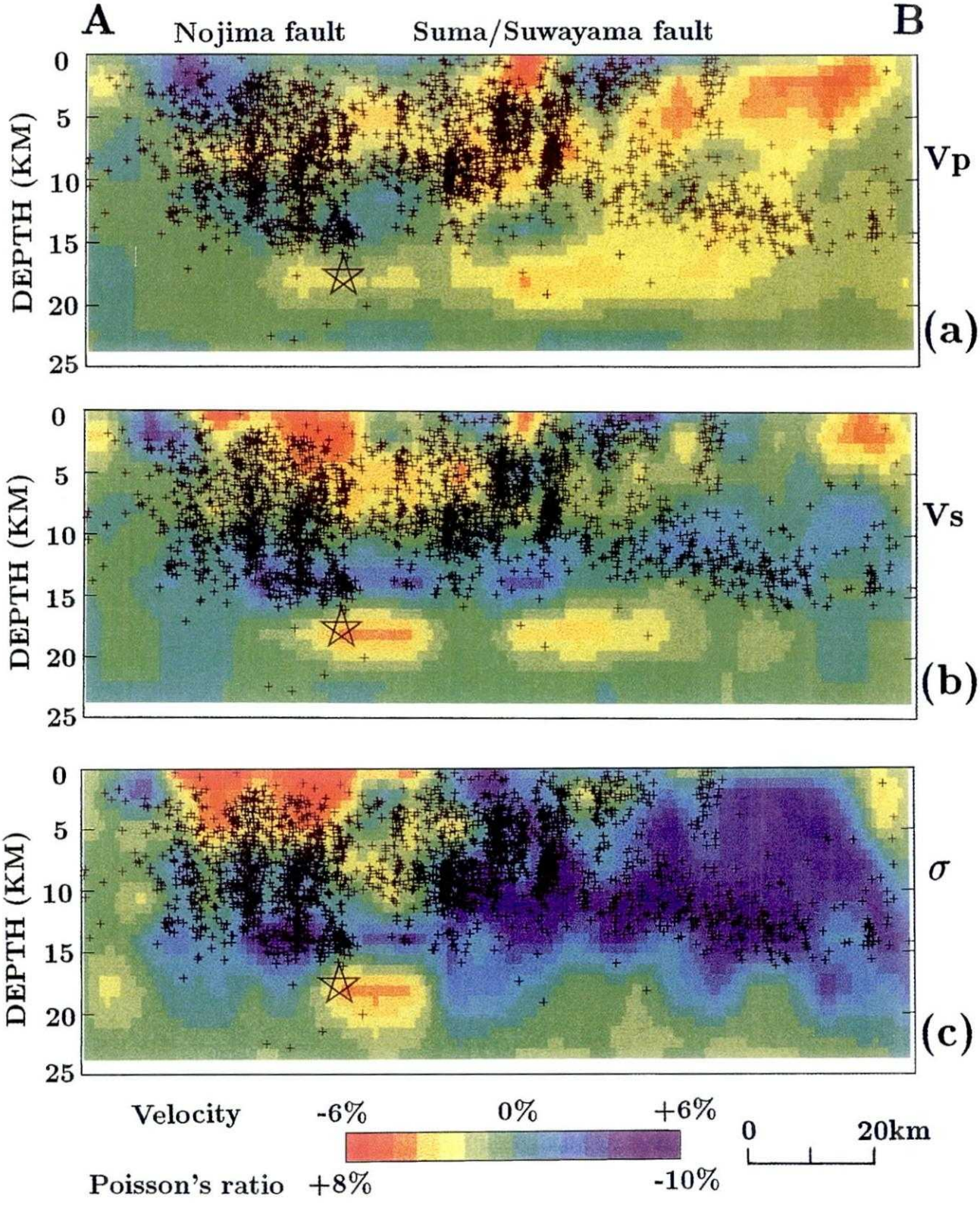

Fig. 9. Vertical cross-sections of (a) *P*-wave velocity (*Vp*), (b) *S*-wave velocity (*Vs*), and (c) Poisson's ratio (σ) along the Kobe fault zone. Slow velocity and high Poisson's ratio are shown in red; fast velocity and low Poisson's ratio are shown in blue. *Vp* and *Vs* perturbations range from -6% to 6% from the average 1-D velocity model. Poisson's ratio ranges from 0.225 to 0.27 (-10% to 8% from the average value). Small crosses denote the Kobe aftershocks within a 6-km width along the Kobe fault zone. Star denotes the hypocenter of the Kobe mainshock; its focal depth is 17 km. The vertical exaggeration is 2 : 1.

sity and the saturation rate in the Kobe fault zone by applying the partial saturation crack model of O'Connell and Budiansky (1974) to the 3-D P and S velocity and Poisson's ratio data obtained from the tomographic inversions by Zhao and Negishi (1998). The crack density parameter (ε) is defined as the product of the number of circular cracks per unit volume and the cube of the average radius of the cracks. The saturation rate (ξ) is defined as the ratio of the number of cracks filled with fluids to the total number of cracks (O'Connell and Budiansky, 1974). Their results show that ε is in the range of 0.02 to 0.15, and ξ is from 20 to 90% in the Kobe area. At the mainshock hypocenter, ε exhibits its maximum value of 0.15 and ξ reaches to 90%, which are 5-10 times greater than those of the surrounding areas off the fault zone.

A significant discrepancy exists between ε and ξ beneath Osaka Bay where the crack density is low but the saturation rate is high (see the color figures in Zhao and Mizuno, 1999). ξ is generally high beneath seas but low beneath land areas. The reason for this difference is not clear. An apparent explanation is that sea waters could permeate down to the deep crust during the long geological history. Note that Osaka Bay and the present sea/land distribution in southwest Japan have existed for two million years (Taira and Nakamura, 1986). This period is long enough for sea water to permeate down to the deep crust through many active faults there, such as the Osaka Bay fault and Nojima fault, which would have been ruptured during many earthquakes cycles in the past two million years. Note that the crustal earthquake cycle is 1,000-2,000 years in the Kobe region (Taira and Nakamura, 1986). In addition to the tomographic results, however, we still need other observational evidence to confirm this scenario.

3. 3. Fluids from slab dehydration

Kobe is located in the forearc region of the Nankai subduction zone. To unravel the structure of the subducting Philippine Sea slab and its possible effect on the Kobe earthquake, Zhao *et al.* (2000a) determined the detailed 3-D velocity structure of the crust and upper mantle under Shikoku and Chugoku (Fig. 10). The subducting Philippine Sea slab is imaged clearly with a thickness of 30-35 km and a P-wave velocity 4-6% higher than that of the normal mantle. Intermediate-depth earthquakes occur within the high-velocity slab. Slow velocity anomalies are visible in the crust and mantle wedge beneath the Kannabe Quaternary volcano and above the subducting slab (Fig. 10), indicating that the Kannabe volcano was caused by the dehydration of the Philippine Sea slab and convective circulation process in the mantle wedge, similar to the active arc volcanoes in northeast Japan.

A prominent low-V zone exists in the lower crust (16-30 km depth) beneath Kii Channel and Awaji Island, directly above the subducted Philippine Sea slab (Fig. 10). This low-V zone has the properties of the anomaly at the Kobe hypocenter, which was detected by the high-resolution imaging, which shows low Vp, low Vs, and high Poisson's ratio (Zhao *et al.*, 1996). Two inversions were conducted to confirm this feature (Zhao *et al.*, 2000a). One uses data from earthquakes that occurred from 1985 to 1994, the other uses data from earthquakes that occurred after the 1995 Kobe earthquake. Both of the inversion results clearly depict the same low-V anomaly under Awaji Island and above the Philippine Sea slab (Fig. 10), indicating that the low-V anomaly existed before the 1995 Kobe earthquake.

These results suggest that the fluids that may have contributed to the initiation of the 1995 Kobe earthquake (Zhao *et al.*, 1996) may be related to the dehydration process of the subducted Philippine Sea slab, in addition to the shallow origins such as meteoric water, pore fluids and mineral dehydration in the crust (Kerrich *et al.*, 1984; Zhao and Mizuno, 1999). The Philippine Sea plate is descending at a very small dip angle in Shikoku and eastern Kii Peninsula, and the subducting slab is located directly under the crust (Fig. 11), thus the fluids from the slab dehydration may easily rise to the crust. When the fluids enter the active faults in the crust (such as the Nojima Fault), fault zone frictions decrease, thus fault ruptures may be triggered to generate large crustal earthquakes (Fig. 7).

This scenario is also supported by geochemical studies. The helium isotope ratio, $^3He/^4He$, is uniformly high in the volcanic areas on the Japan Islands, which is interpreted to be associated with the diapiric uprise of magmas resulting from the dehydration process of the subducting Pacific and Philippine Sea slabs (Sano and Wakita, 1985). In Kobe, Osaka and western Kii Peninsula where no volcano exists, however, high values for the helium isotope

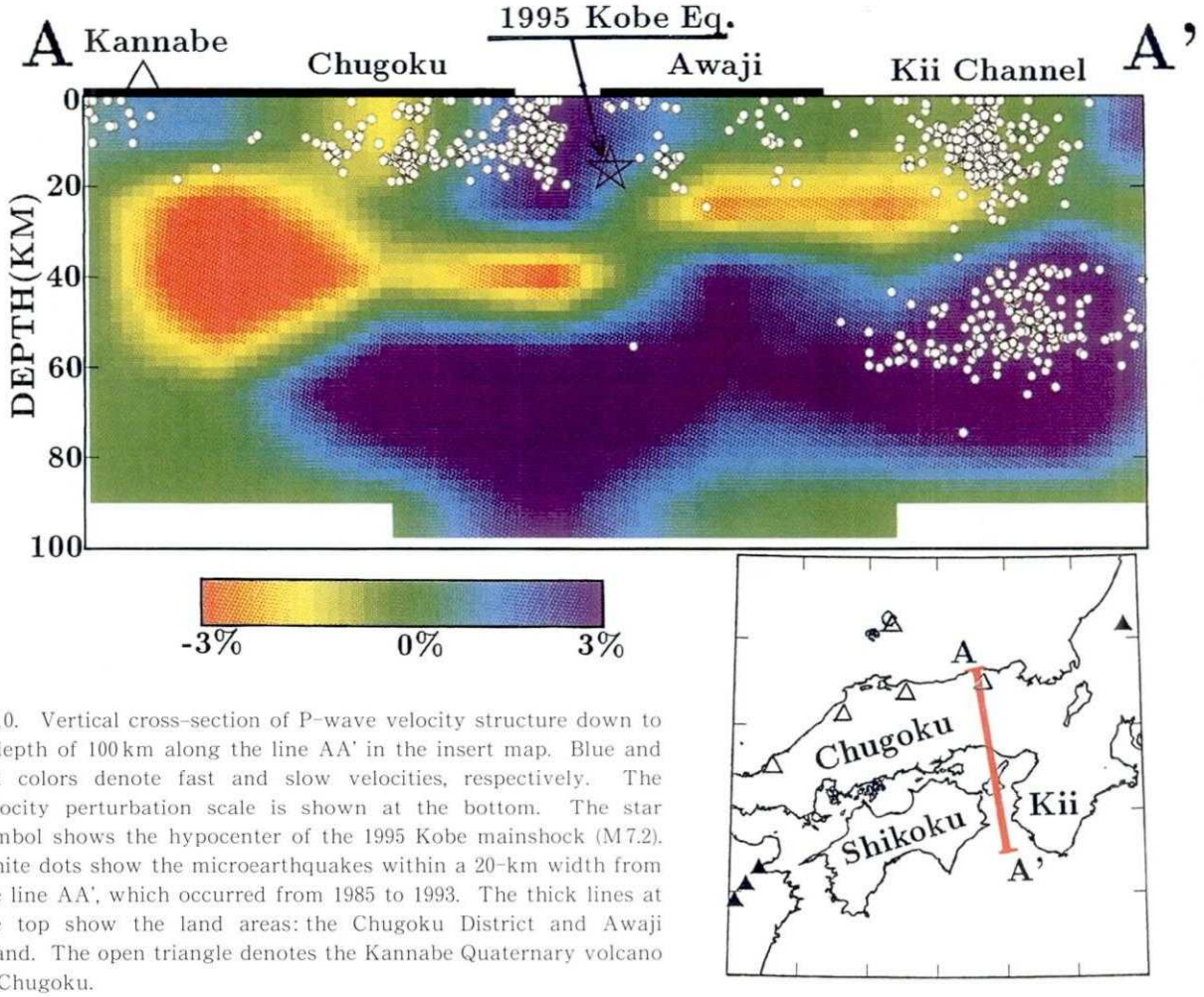

Fig. 10. Vertical cross-section of P-wave velocity structure down to a depth of 100 km along the line AA' in the insert map. Blue and red colors denote fast and slow velocities, respectively. The velocity perturbation scale is shown at the bottom. The star symbol shows the hypocenter of the 1995 Kobe mainshock (M 7.2). White dots show the microearthquakes within a 20-km width from the line AA', which occurred from 1985 to 1993. The thick lines at the top show the land areas: the Chugoku District and Awaji Island. The open triangle denotes the Kannabe Quaternary volcano in Chugoku.

ratio were also observed (Wakita *et al.*, 1987), suggesting that volatiles from the slab dehydration containing helium with a high $^{3}He/^{4}He$ ratio have risen up to the crust and the Earth surface. Similar geochemical results are also obtained for the forearc region in southern Italy where melts and fluids from the dehydration of the subducting Adriatic plate may have intruded into the active lithospheric faults and thus affect the genesis of large crustal earthquakes (Italiano *et al.*, 2000).

From seismic reflection and geoelectricity prospectings in western Canada, Hyndman (1988) found a dipping zone of trapped free pore water in the lower crust under the Cascadia forearc region. The free water is interpreted to be generated by the dehydration of the subducting Juan der Fuca slab associated with the transformation of metabasalt to eclogite, which is also imaged by a tomographic imaging (Zhao *et al.*, 2001).

4. The 2001 Geiyo earthquake: Slab rupture and dehydration

The 24 March 2001 Geiyo earthquake (M 6.4) occurred at a depth of 50 km under the Seto Inland Sea and caused two dead, hundreds injured, and tremendous property losses (Japan Meteorological Agency, 2001) (Fig. 12). The earthquake was generated by a normal faulting under an east-west tensional stress regime. The seismogenic fault is north-south oriented and dips toward the west with a dip angle of 35° from the vertical. Aftershocks are distributed along the N-S oriented fault zone with a length of approximately 30 km. The mainshock hypocenter is located at the northern end of the aftershock zone. It is considered that the Geiyo earthquake was caused by a tensional fracture of the subducted Philippine Sea slab (Japan Meteorological Agency, 2001).

Recently, a high-quality and dense broad-band

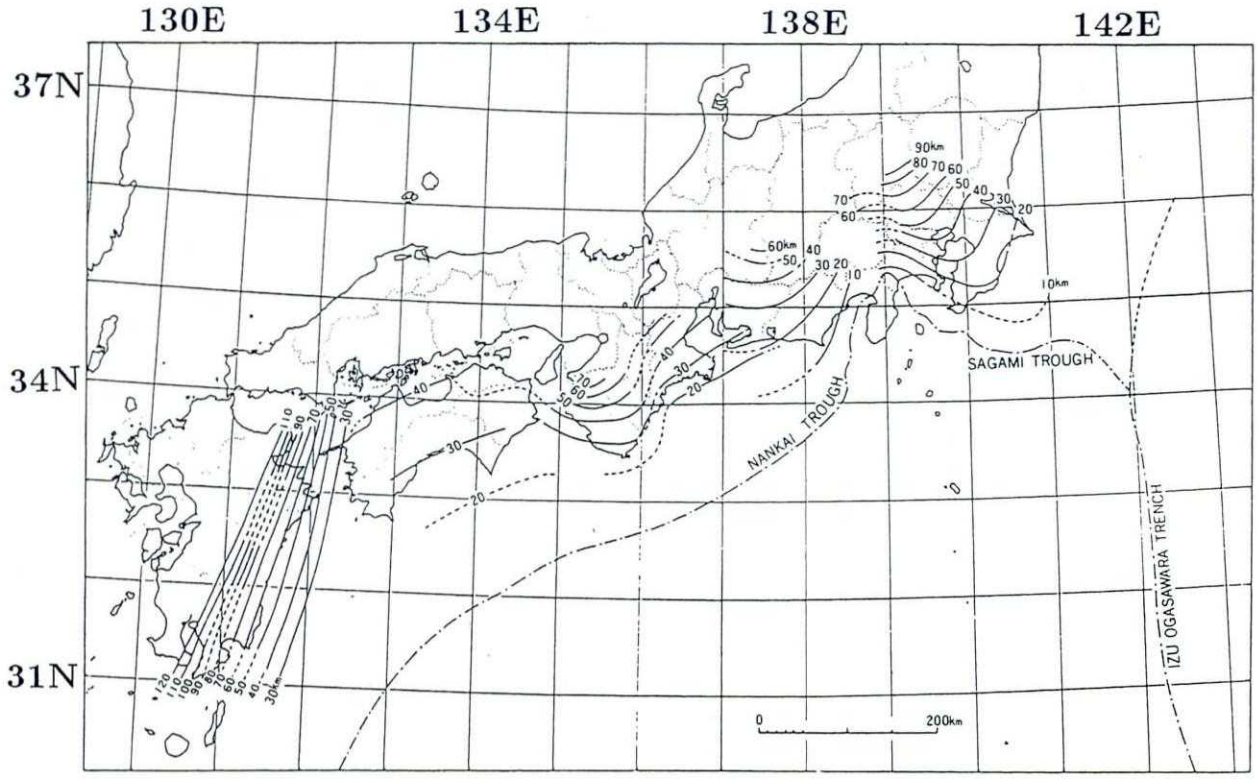

Fig. 11. Upper boundary of the subducting Philippine Sea plate beneath southwest Japan as derived from hypocentral distribution of intermediate-depth earthquakes (after Ishida, 1992).

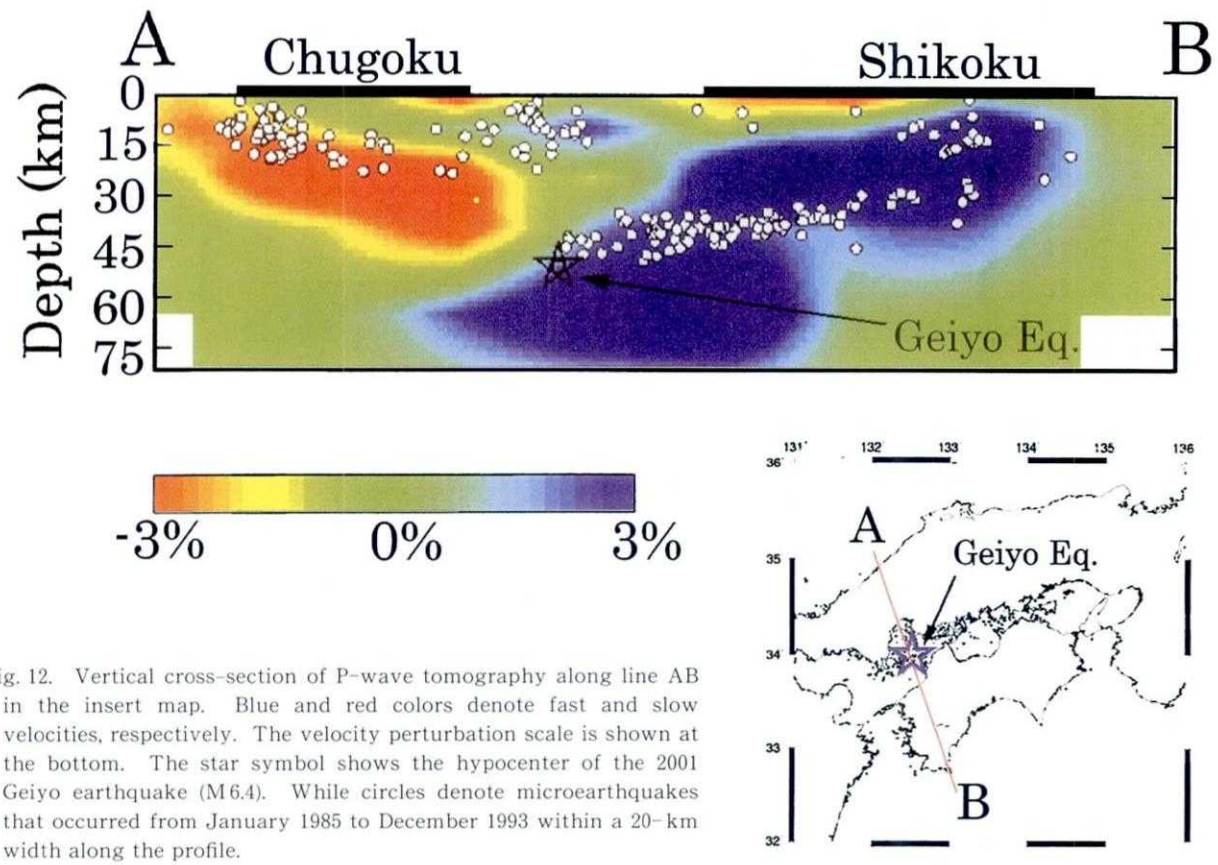

Fig. 12. Vertical cross-section of P-wave tomography along line AB in the insert map. Blue and red colors denote fast and slow velocities, respectively. The velocity perturbation scale is shown at the bottom. The star symbol shows the hypocenter of the 2001 Geiyo earthquake (M 6.4). While circles denote microearthquakes that occurred from January 1985 to December 1993 within a 20-km width along the profile.

seismic network, Hi-net, has been installed on the Japan Islands by the National Research Institute for Earth Science and Disaster Prevention (Obara *et al.*, 2000). The Hi-net stations are installed in areas that are not well covered by the Japan University Seismic Network (Fig. 1.). Now the Hi-net and the university networks cover the Japan Islands densely and uniformly with a station spacing of about 20 km. Recently, we have used about 45,000 P and S arrival times from 876 shallow and intermediate-depth earthquakes (0-80 km depth) recorded by Hi-net from October 1999 to December 2000 to determine the 3-D velocity structure of southwest Japan (Fig. 5, 12). The subducting Philippine Sea slab is clearly imaged as high-V zones under Shikoku Island and Kii Peninsula. Prominent low-V zones are visible along the Japan Sea coast in the upper crust (Fig. 5a) and under the northern part of Chugoku region in the lower crust (Fig. 5b). In the upper mantle wedge the low-V zones are shifted toward the south under Chugoku (Fig. 5c). In the cross-sectional view (Fig. 12), we can see the low-V zone dipping toward the south. In the north the low-V zone is connected to the volcanic front at the Japan Sea coast of the Chugoku region, while to the south it extends to a depth of about 50 km, directly above the subducted Philippine Sea slab (Fig. 12). Apparently, the low-V zone represents a high-temperature anomaly containing magmas caused by dehydration of the subducted slab and convective circulations of the mantle wedge, as observed previously in other subduction zones (e.g., Zhao *et al.*, 1992; 1995, 1997b, 2001). Under Shikoku, intermediate-depth earthquakes seem to occur in the central to lower portions of the high-velocity Philippine Sea slab (Fig. 12). The lower part of the slab was not imaged well, because few rays from the local events pass that area. A better image may be obtained by adding regional and teleseismic rays.

The Geiyo mainshock hypocenter is located where the mantle-wedge low-V zone is nearly connected to the subducting Philippine Sea slab, where slab dehydration should be active (Fig. 13a). In addition, very few intermediate-depth earthquakes occur north of the Geiyo mainshock hypocenter (Japan Meteorological Agency, 2001). Hence the Geiyo hypocenter may just represent the northern edge of the seismic portion of the Philippine Sea slab, where the

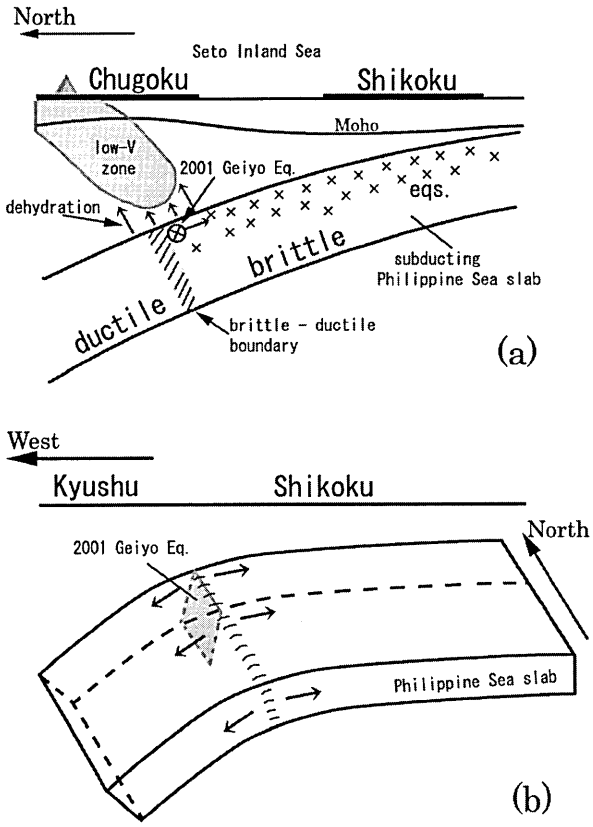

Fig. 13. Schematic illustration of the cause of the 2001 Geiyo earthquake (M 6.4). See text for details.

brittle to ductile transformation may take place in the slab. These features suggest that the 2001 Geiyo earthquake may be related to structural anomalies associated with the dehydration and the brittle to ductile transformation of the subducting Philippine Sea slab.

The geometry of the subducting Philippine Sea slab changes around the epicentral area of the Geiyo earthquake (Fig. 11, 13b). The slab is flat under Shikoku, but steeply dips toward the west under Kyushu. The local stress regime of the east-west extension in the Geiyo earthquake area may be associated with the curvature of the Philippine Sea slab between Shikoku and Kyushu. The occurrence of the 2001 Geiyo earthquake may be caused by the joint effects of the local tensional stress regime, structural heterogeneities related to the brittle to ductile transformation within the slab, and the strength weakening and triggering effects due to slab dehydration.

5. Slab boundary heterogeneity and interplate earthquakes

The majority of earthquakes in subduction zones occur along the interplate thrust zone between the subducting oceanic plate and the overriding continental plate. The frequent occurrences of great thrust earthquakes have caused widespread damage to coastal areas through strong shakings and tsunamis. Information on the detailed structure of the forearc region of subduction zones is crucial for our understanding of the initiation of subduction, the interplate seismic coupling and the rupture nucleation of destructive interplate earthquakes. However, such information is very scanty, because the forearc regions are generally covered under oceans, so there are few seismic stations available. Observations with ocean bottom seismometers are very expensive and are limited in both time and space (e.g., Ito *et al.*, 2000 ; Hino *et al.*, 2000).

Recently, we attempted to investigate the 3-D velocity structure under the Pacific Ocean between the Japan Trench and the Pacific Coast of Northeast (NE) Japan. We used two groups of earthquakes (Fig. 14). One group consists of 1,216 shallow and intermediate-depth earthquakes, which occurred beneath the NE Japan land area, therefore they were located well by the seismic network. The other group consists of 598 earthquakes that occurred under the Pacific Ocean, whose hypocentral locations were determined well by Umino *et al.* (1995) with sP depth phases (radiated upward as an S-wave from an earthquake under the Pacific Ocean, reflected at the ocean floor and at the same time converted into P-wave, and then recorded by a seismometer on the land area). The total of 1,814 events were recorded by the dense seismic network of Tohoku University, which covers the NE Japan land area (Fig. 1.). The 1,216 events under the land area were also recorded by the temporary seismic stations deployed in central Tohoku during 1997-1998 (Hasegawa and Hirata, 1999). We applied the tomography method of Zhao *et al.* (1992) to 86,024 P and 47,756 S wave arrival times from the 1,814 events to determine tomographic images for the whole NE Japan arc from the Japan Trench to the Japan Sea coast. The 1,216 events under the land area were relocated in the inversion process, while the hypocentral parameters of the 598 events under the Pacific Ocean determined by Umino *et al.* (1995) were fixed during the inversion process.

Fig. 15 shows the depth distribution of the upper boundary of the subducting Pacific plate under the NE Japan arc (Zhao *et al.*, 1997a). Fig. 16 shows the P-wave tomographic image along the upper boundary of the Pacific plate (Fig. 15). There are strong lateral heterogeneities in the slab boundary (Fig. 16). Between 38.7° and 39.8° north latitude, an east-west oriented low-V feature is visible from the Pacific coast under Sanriku to the Japan Trench. Around the low-V zone, several slow and ultra-slow large earthquakes occurred (Kawasaki *et al.*, 2001). A north-south oriented low-V zone of 30-40 km in width is visible off the Pacific coast and parallel to the Japan Trench, which is consistent with a forearc dehydration zone appearing in the numerical simulation results of Iwamori (1998). Comparing the tomographic image along the slab boundary with the distribution of large interplate earthquakes (M 7.0-8.5), we found that most of the interplate earthquakes occur outside the low-V zones (Fig. 16). The low-V zones may represent decoupled areas, perhaps containing fluids. Most of the large interplate earthquakes are located in areas with velocities higher than the average, which may represent strong-coupled asperities. S-wave velocity and Poisson's ratio images are also determined along the slab boundary, but have a lower resolution. More S-wave data will be collected to image Vs and Poisson's ratio, which would provide plenty of information on physical properties and fluid contents in the slab boundary, and their effects on interplate seismic coupling.

Husen *et al.* (2000) determined Vp and Vp/Vs tomographic images in the forearc region of north Chile, where the great Antofagasta earthquake (M 8.0) occurred on July 30, 1995. They detected a zone of high Vp/Vs ratio within the rupture area of the Antofagasta mainshock, just above the subducted slab. They interpreted that the high Vp/Vs ratio indicates postseismic fluid migration from the subducted oceanic crust into the overlying lower crust. But it is also possible that fluids on the slab boundary might have triggered the rupture of the great Antofagasta earthquake.

These results suggest that lateral heterogeneities (strong coupled sections or asperities and weakly coupled or decoupled patches probably containing fluids) exist along the slab boundary, which may control the degree and the spatial extent of the interplate seismic coupling and the rupture nucleation of

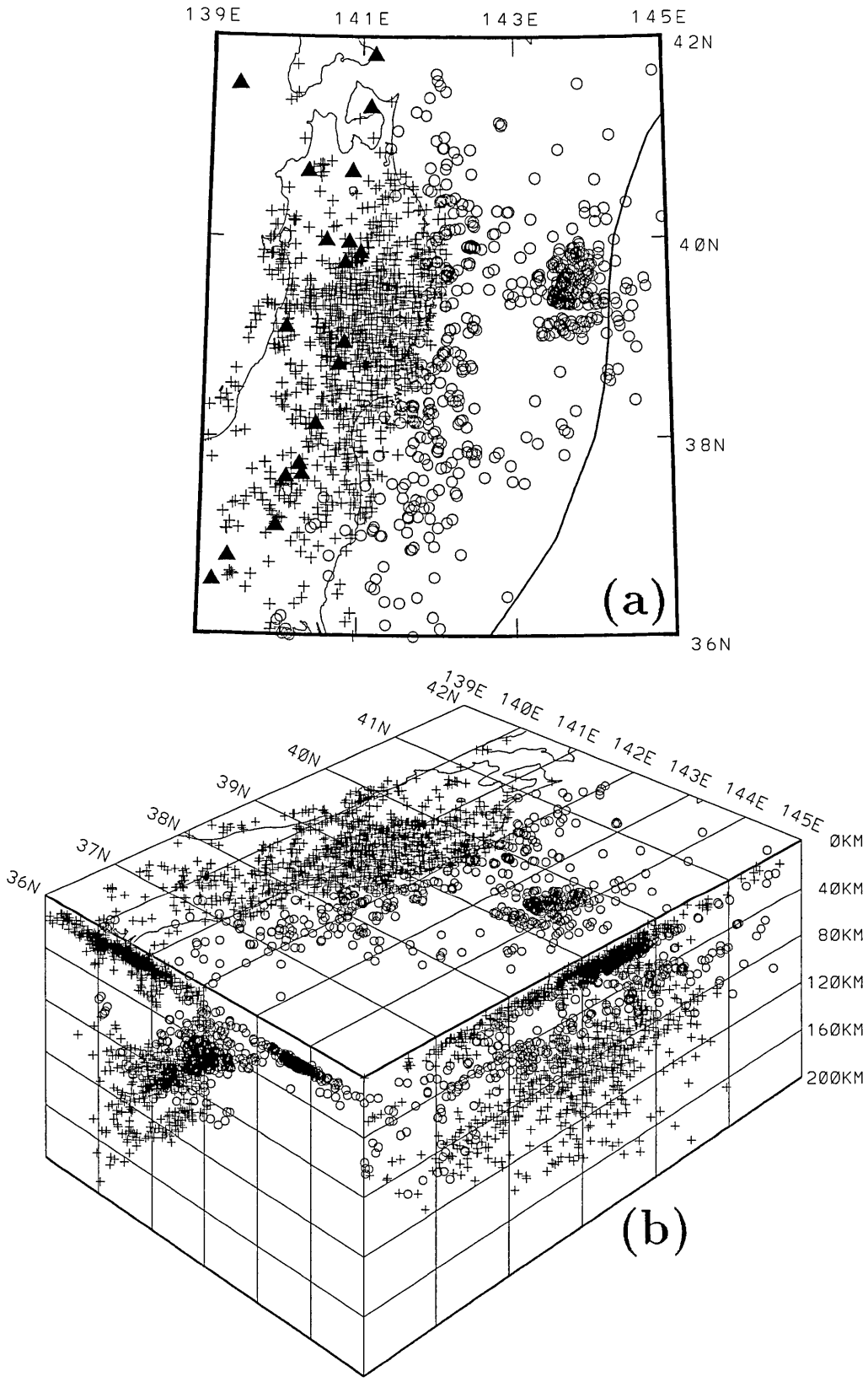

Fig. 14. Plan view (a) and three-dimensional view (b) of the distribution of 1,814 earthquakes used in the tomographic inversion of the northeast Japan forearc region. Circles denote 598 events that were located well with sP depth phase data. Crosses denote 1,216 events that were locately by the land seismic network. The curved line and solid triangles in (a) show the location of Japan trench and active arc volcanoes, respectively.

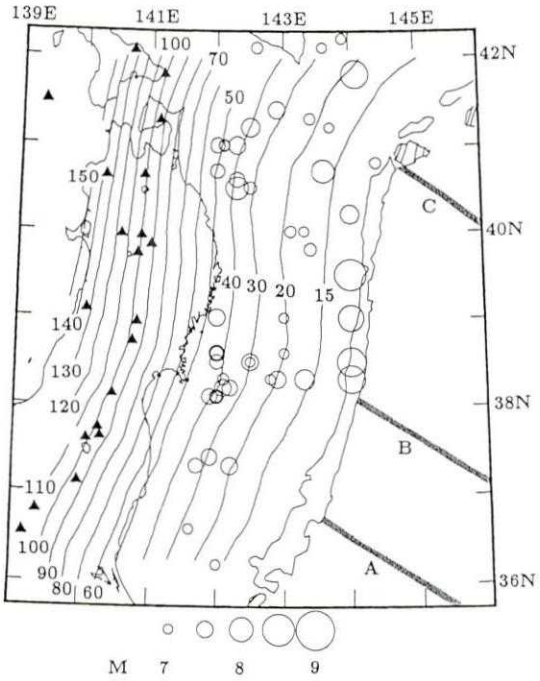

Fig. 15. Depth distribution of the upper boundary of the subducted Pacific plate beneath northeastern Japan (Zhao *et al.*, 1997a). The slab boundary deeper than 45 km is determined with SP converted waves; shallower than 45 km, it is estimated from earthquakes below the Pacific Ocean located well with sP depth phases. Numerals attached to the contours indicate the depths in kilometers. Hatched areas (A, B and C) denote the oceanic fracture zones. Active volcanoes are shown by solid triangles. Open circles denote large historic interplate earthquakes that occurred from 830 to 1995, with magnitudes equal to or greater than 7.0 and focal depths shallower than 60 km. The magnitude scale is shown at the bottom. Note that the contour line showing the Japan Trench has a water depth of 7,000 m.

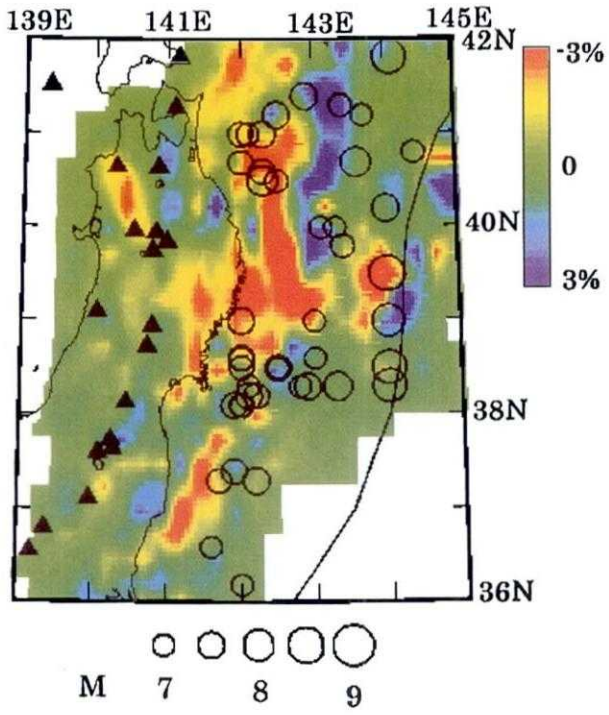

Fig. 16. P-wave tomography along the upper boundary of the subducting Pacific plate (Fig. 15). Blue and red colors denote fast and slow velocities, respectively. The velocity perturbation scale is shown to the right. Open circles denote large historic interplate earthquakes that occurred from 830 to 1995, with magnitudes equal to or greater than 7.0 and focal depths shallower than 60 km. The magnitude scale is shown at the bottom. The curved line and solid triangles denote the Japan trench and active arc volcanoes, respectively.

thrust earthquakes. The occurrence of slow and ultra-slow large thrust earthquakes (Kawasaki *et al.*, 2001) may be closely related to the fluid contents along the slab boundary.

6. Discussion and Conclusions

Fluids exist widely in the crust and uppermost mantle in the forearc regions of subduction zones (Tatsumi, 1989; Peacock, 1990; Iwamori, 1998). The existence of fluids beneath the seismogenic layer may affect the long-term structural and compositional evolution of the fault zone, change the strength of the fault zone, and alter the local stress regime (Sibson, 1992; Hickman *et al.*, 1995). These influences may enhance stress concentration in the seismogenic layer leading to mechanical failure. Spatial and temporal variations in the crustal stress field have been reported for the source areas of the Kobe earthquake (Katao *et al.*, 1997) and the 1994 Northridge earthquake (M 6.7) in southern California (Zhao *et al.*, 1997c), which have been associated with fluids in the fault zones.

As described above, we attributed the seismic velocity variations mainly to temperature changes in the volcanic areas and to fluids in the forearc regions in southwest Japan. In the forearc areas of Hokkaido and eastern Honshu, where the Pacific plate is subducting, there may also be effects of fluids from the dehydration of the Pacific slab. Heat flow and geothermal gradient are lower in the Pacific coast areas, and so lower temperatures are expected there. Lithological variations in the crust may also contribute to

the heterogeneity of material properties and stress field, and cause the slow seismic velocity and the weakening of the seismogenic layer (Magistrale and Zhou, 1996). To distinguish the effects of magma, fluids, and lithological changes on the seismic velocity, much future work is needed using and combining different geophysical imaging methods (such as gravity, magnetotelluric, geoelectric, geothermal, and seismic investigations), numerical simulations, and laboratory experiments. Future theoretical and experimental work of seismology should pay more attention to the inelastic structure and processes (magma, fluids and their migrations) in the Earth's interior.

Hauksson and Haase (1997) found that four earthquakes ($M>5.9$) in the Los Angeles basin area occurred in or adjacent to high-velocity zones. They interpreted that the high-velocity zones form the upper block of a thrust fault or a thin skinned structure, i.e., the earthquake ruptures actually happened at the boundary between high- and low-velocity zones, as shown in their Fig. 13. Hence their results for Southern California do not contradict our observations in Japan. The tectonic background is very different between Japan and California (e.g., there is no active volcano in California), which would also cause differences in the earthquake dynamics and in the relationship between tomography and earthquake distribution.

The 1995 Kobe earthquake has a right-lateral strike-slip focal mechanism caused by an east-west compressional stress field, and so it is generally considered that the subduction of the Philippine Sea plate makes little contribution to the generation of the Kobe earthquake. However, our present work shows that the Philippine Sea slab may have contributed to the Kobe earthquake through chemical and mechanical processes such as dehydration and fluid flow, instead of providing the driving stress. If this is true, it is important from the viewpoint of hazard mitigation, to detect the fluid-related anomalies in the fault zones in forearc areas of subduction regions.

The many pieces of evidence mentioned above suggest that the generation of a large earthquake is not a pure mechanical process, but is closely related to the physical and chemical properties of materials in the crust and upper mantle, such as magma and fluids. The rupture nucleation zone should have a three-dimensional spatial extent, not just limited to the two-dimensional surface of a fault, as suggested earlier by Tsuboi (1956) in the concept of *earthquake volume*. Complex physical and chemical reactions may take place in the source zone of a future earthquake, causing heterogeneities in the material property and stress field, which may be detected using seismic tomography and other geophysical methods. The source zone of a M6 to 8 earthquake extends from about 10 km to over 100 km (Kanamori and Anderson, 1975). The resolution of our tomographic imaging is close to that scale of the earthquake sources, which may have enabled us to image the earthquake-related heterogeneities (i.e., earthquake volumes) in the crust and the uppermost mantle in Japan.

These results indicate that large earthquakes do not strike anywhere, but only in anomalous areas that may be detected using geophysical methods. Higher-resolution seismic imaging and combining seismological studies with geological, geochemical, and geophysical investigations would certainly provide us with a better understanding of the earthquake generating process, and would also contribute to the mitigation of earthquake hazards.

Acknowledgements

This work was partially supported by a grant from Japan Society for the Promotion of Science (Kiban-B No.11440134). The authors thank K. Asamori, F. Ochi, A. Kurogi, T. Nishino and T. Ono for their assistance at the data processing stages and for useful discussion.

References

Asamori, K. and D. Zhao, 2001, Imaging magma chambers under Unzen Volcano, submitted to *Geophys. Res. Lett.*

Hasegawa, A. and N. Hirata, 1999, Transect of Northeast Japan: Island arc deformation and crustal activity, *Earth Monthly*, **27**, 5-11.

Hasegawa, A. and A. Yamamoto, 1994, Deep, low-frequency microearthquakes in or around seismic low-velocity zones beneath active volcanoes in northeastern Japan, *Tectonophysics*, **233**, 233-252.

Hasegawa, A. and D. Zhao, 1994, Deep structure of island arc magmatic regions as inferred from seismic observations, in *Magmatic Systems*, edited by M.P. Ryan, pp. 179-193, Academics, San Diego, Calif.

Hasegawa, A., A. Yamamoto, N. Umino, S. Miura, D. Zhao, and H. Sato, 2000, Seismic activity and deformation process of the overriding plate in the northeastern Japan subduction zone, *Tectonophysics*, **319**, 225-239.

Hauksson, E. and J. Haase, 1997, Three-dimensional Vp and Vp/Vs velocity models of the Los Angeles basin and central Transverse Ranges, California, *J. Geophys. Res.*, **102**, 5423-5453.

Hickman, S., R. Sibson, and R. Bruhn, 1995, Introduction to special section: Mechanical involvement of fluids in faulting, *J. Geophys. Res.*, **100**, 12831-12840.

Hino, R. *et al.*, 2000, Aftershock distribution of the 1994 Sanriku-oki earthquake (Mw 7.7) revealed by ocean bottom seismographic observation, *J. Geophys. Res.*, **105**, 21697-21710.

Hiramatsu, Y., M. Ando, T. Tsukada, and T. Ooida, 1998, Three-dimensional image of the anisotropic bodies beneath central Honshu, Japan, *Geophys. J. Int.*, **135**, 801-816.

Horiuchi, S., N. Tsumura, and A. Hasegawa, 1997, Mapping of a magma reservoir beneath Nikko-Shirane volcano in northern Kanto, Japan, from travel time and seismogram shape anomalies, *J. Geophys. Res.*, **102**, 18071-18090.

Husen, S., E. Kissling and E. Flueh, 2000, Local earthquake tomography of shallow subduction in north Chile: A combined onshore and offshore study, *J. Geophys. Res.*, **105**, 28183-28198.

Hyndman, R.D., 1988, Dipping seismic reflectors, electrically conductive zones, and trapped water in the crust over a subducting plate, *J. Geophys. Res.*, **93**, 13391-13405.

Iidaka, T. and K. Obara, 1994, Shear-wave polarization anisotropy in the upper mantle from a deep earthquake, *Phys. Earth Planet. Inter.*, **82**, 19-25.

Iidaka, T., K. Miura and A. Ikami, 1993, Evidence for the existence of a mid-crustal reflector in the Beppu-Shimabara graben, Kyushu, Japan, Geophys. Res. Lett., **20**, 1699-1702.

Ishida, M., 1992, Geometry and relative motion of the Philippine Sea plate and Pacific plate beneath the Kanto-Tokai district, Japan, *J. Geophys. Res.*, **97**, 489-513.

Italiano, F., M. Martelli, G. Martinelli and P. Nuccio, 2000, Geochemical evidence of melt intrusions along lithospheric faults of the Southern Apennines, Italy: Geodynamic and seismogenic implications, *J. Geophys. Res.*, **105**, 13569-13578.

Ito, K., 1993, Cutoff depth of seismicity and large earthquakes near active volcanoes in Japan, *Tectonophysics*, **217**, 11-21.

Ito, S. *et al.*, 2000, Deep seismic structure of the seismogenic plate boundary in the off-Sanriku region, northeastern Japan, *Tectonophysics*, **319**, 261-274.

Iwamori, H., 1998, Transportation of H_2O and melting in subduction zones, *Earth Planet. Sci. Lett.*, **160**, 65-80.

Japan Meteorological Agency, 2001, Earthquake report (February-March 2001), *Seismological Society of Japan Newsletter*, **13**, 18-22.

Kanamori, H., and D. Anderson, 1995, Theoretical basis of some empirical relations in seismology, *Bull. Seismol. Soc. Am.*, **65**, 1073-1095.

Katao, H., N. Maeda, Y. Hiramatsu, Y. Iio, and S. Nakao, 1997, Detailed mapping of focal mechanisms in and around the 1995 Hyogo-Ken Nanbu earthquake rupture zone, *J. Phys. Earth*, **45**, 105-119.

Kawasaki, I., Y. Asai and Y. Tamura, 2001, Space-time distribution of interplate moment release including slow earthquakes and the seismo-geodetic coupling in the Sanriku-oki region along the Japan trench, *Tectonophysics*, **330**, 267-283.

Kerrich, R., T. La Tour, and L. Willmore, 1984, Fluid participation in deep fault zones: Evidence from geological, geochemical, and $^{18}O/^{16}O$ relations, *J. Geophys. Res.*, **89**, 4331-4343.

Komazawa, M. and H. Kamata, 1985, The basement structure of the Hohi geothermal area obtained by gravimetric analysis in central-north Kyushu, Japan, *Rep. Geol. Surv. Jpn.*, **264**, 305-333.

Magistrale, H. and H. Zhou, 1986, Lithologic control of the depth of earthquakes in southern California, *Science*, **273**, 639-642.

Matsumoto, S. and A. Hasegawa, 1986, Distinct S wave reflector in the midcrust beneath Nikko-Shirane volcano in the northeastern Japan arc, *J. Geophys. Res.*, **101**, 3067-3083.

Obara, K., S. Hori and K. Kasahara, 2000, Hi-net: Data acquisition, processing and public use system, *Program and Abstracts, 2000 Annual Meeting of the Seismological Society of Japan*, November 20-22, 2000, Tsukuba.

O'Connell, R. and B. Budiansky, 1974, Seismic velocities in dry and saturated cracked solids, *J. Geophys. Res.*, **79**, 5412-5426.

Ohmi, S. and J. Lees, 1995, Three-dimensional P- and S-wave velocity structure below Unzen volcano, *J. Volcanol. Geotherm. Res.*, **65**, 1-26.

Okada, T., T. Matsuzawa, and A. Hasegawa, 1995, Shear-wave polarization anisotropy beneath the north-eastern part of Honshu, Japan, *Geophys. J. Int.*, **123**, 781-797.

Okubo, Y., H. Tsu, and K. Ogawa, 1989, Estimation of Curie point temperature and geothermal structure of island arcs of Japan, *Tectonophysics*, **159**, 279-290.

Peacock, S., 1990, Fluid processes in subduction zones, *Science*, **248**, 329-345.

Sano, Y. and H. Wakita, 1985, Geographical distribution of $^3He/^4He$ ratios in Japan: Implications for arc tectonics and incipient magmatism, *J. Geophys. Res.*, **90**, 8729-8741.

Sekiguchi, S., 1991, Three-dimensional Q structure beneath the Kanto-Tokai district, Japan, *Tectonophysics*, **195**, 83-104.

Seno, T., T. Sakurai, and S. Stein, 1996, Can the Okhotsk plate be discriminated from the North American plate? *J. Geophys. Res.*, **101**, 11305-11315.

Seno, T., S. Stein, and A. Gripp, 1993, A model for the motion of the Philippine Sea plate consistent with NUVEL-1 and geological data, *J. Geophys. Res.*, **98**, 17941-17948.

Sibson, R.H., 1992, Implications of fault-valve behavior for rupture nucleation and recurrence, *Tectonophysics*, **211**, 283-293.

Suyehiro, K., 1988, Structure beneath Unzen volcano, *Bull. Volcanol. Soc. Jpn.*, **33**, 134-136.

Taira, A. and K. Nakamura, 1986, *The formation of the Japanese Islands*, **414** pp., Iwanami Press, Tokyo.

Tatsumi, Y., 1989, Migration of fluid phases and genesis of basalt magmas in subduction zones, *J. Geophys. Res.*, **94**, 4697-4707.

Tsuboi, C., 1956, Earthquake energy, earthquake volume,

aftershock area, and strength of the earth's crust, *J. Phys. Earth*, **4**, 63-66.

Tsuboi, S., K. Koketsu, K. Takano, T. Miyatake, K. Abe, and Y. Hagiwara, 1989, Hypocenter determination procedure of Japan University Network Earthquake Catalog, *J. Seismol. Soc. Japan*, **42**, 277-284.

Tsumura, N., S. Matsumoto, S. Horiuchi and A. Hasegawa, 2000, Three-dimensional attenuation structure beneath the northeastern Japan arc estimated from spectra of small earthquakes, *Tectonophysics*, **319**, 241-260.

Umino, N., Hasegawa, A. and Matsuzawa, T., 1995, sP depth phase at small epicentral distances and estimated subducting plate boundary, *Geophys.* J. Int., **120**, 356-366.

Usami, T., 1999, *Catalog of damaging earthquakes in Japan*, University of Tokyo Press, 493 pp., Tokyo.

Utsu, T., 1982, Catalog of large earthquakes in the region of Japan from 1885 through 1980 (in Japanese), *Bull. Earthq. Res. Inst., Univ. Tokyo*, **57**, 401-463.

Wakita, H., Y. Sano and M. Mizoue, 1987, High ^{3}He emanation and seismic swarms observed in a nonvolcanic, forearc region, *J. Geophys. Res.*, **92**, 12539-12546.

Yokoyama, I., S. Aramaki, and K. Nakamura, 1987, *Volcanoes*, 294 pp., Iwanami Press, Tokyo.

Yuhara, K., 1973, Effect of the hydrothermal systems of the terrestrial heat flow (in Japanese), *Bull. Volcanol. Soc. Japan*, **18**, 129-142.

Zhao, D., 2001, Correlation of seismic tomography and large historic earthquakesin Japan from AD 679 to 2000, *Earth Monthly*, **23**, 95-103.

Zhao, D. and A. Hasegawa, 1994, Teleseismic evidence for lateral heterogeneitiesin the northeastern Japan arc, *Tectonophysics*, **237**, 189-199.

Zhao, D. and T. Mizuno, 1999, Crack density and saturation rate in the 1995 Kobe earthquake region, *Geophys. Res. Lett.*, **26**, 3213-3216.

Zhao, D. and H. Negishi, 1998, The 1995 Kobe earthquake: Seismic image of the source zone and its implications for the rupture nucleation, *J. Geophys. Res.*, **103**, 9967-9986.

Zhao, D., A. Hasegawa and S. Horiuchi, 1992, Tomographic imaging of P and S wave velocity structure beneath northeastern Japan, *J. Geophys. Res.*, **97**, 19909-19928.

Zhao, D., A. Hasegawa and H. Kanamori, 1994, Deep structure of Japan subduction zone as derived from local, regional and teleseismic events, *J. Geophys. Res.*, **99**, 22313-22329.

Zhao, D., D. Christensen and H. Pulpan, 1995, Tomographic imaging of the Alaska subduction zone, *J. Geophys. Res.*, **100**, 6487-6504.

Zhao, D., H. Kanamori, H. Negishi and D. Wiens, 1996, Tomography of the source area of the 1995 Kobe earthquake : Evidence for fluids at the hypocenter? *Science*, **274**, 1891-1894.

Zhao, D., T. Matsuzawa and A. Hasegawa, 1997a, Morphology of the subducting slab boundary in the northeastern Japan arc, *Phys. Earth Planet. Inter.*, **102**, 89-104.

Zhao, D., Y. Xu, D. Wiens, L. Dorman, J. Hildebrand and S. Webb, 1997b, Depth extent of the Lau back-arc spreading center and its relation to subduction processes, *Science*, **278**, 254-257.

Zhao, D., H. Kanamori and D. Wiens, 1997c, State of stress before and after the 1994 Northridge earthquake, *Geophys. Res. Lett.*, **24**, 519-522.

Zhao, D., F. Ochi, A. Hasegawa and A. Yamamoto, 2000a, Evidence for the location and cause of large crustal earthquakes in Japan, *J. Geophys. Res.*, **105**, 13579-13594.

Zhao, D., K. Asamori and H. Iwamori, 2000b, Seismic structure and magmatism of the young Kyushu subduction zone, *Geophys. Res. Lett.*, **27**, 2057-2060.

Zhao, D., K. Wang, G. Rogers and S. Peacock, 2001, Tomographic image of low P velocity anomalies above slab in northern Cascadia subduction zone, *Earth Planets Space*, **53**, 285-293.

(Received June 28, 2001)
(Accepted September 17, 2001)